Human liver stem cells improve liver injury in a model of fulminant liver failure.

Herrera Sanchez MB; Fonsato V; Bruno S; Grange C; Gilbo N; Romagnoli R; Tetta C; Camussi G.. Human liver stem cells improve liver injury in a model of fulminant liver failure.. HEPATOLOGY. 57 pp: 311-319.
DOI: 10.1002/hep.25986

Human liver stem cells improve liver injury in a model of fulminant liver failure

Herrera MB, Fonsato V, Bruno S, Grange C, Gilbo N, Romagnoli R, Tetta C, Camussi G.

Abstract

Liver transplantation is currently the only effective therapy for fulminant liver failure, but its use is limited by the scarcity of organs for transplantation, high costs, and lifelong immunosuppression. Here we investigated whether human liver stem cells (HLSCs) protect from death in a lethal model of fulminant liver failure induced by intraperitoneal injection of D-galactosamine and lipopolysaccharide in SCID mice. We show that injection of HLSCs and of HLSC-conditioned medium (CM) significantly attenuates mouse mortality in this model. Histopathological analysis of liver tissue showed reduction of liver apoptosis and enhancement of liver regeneration. By optical imaging we observed a preferential localization of labeled HLSCs within the liver. HLSCs were detected by immunohistochemistry in large liver vessels (at 24 hours) and in the liver parenchyma (after day 3). Fluorescence in situ hybridization analysis with the human pan-centromeric probe showed that positive cells were cytokeratin-negative at 24 hours. Coexpression of cytokeratin and human chromosome was observed at 7 and, to a lesser extent, at 21 days. HLSC-derived CM mimicked the effect of HLSCs in vivo. Composition analysis of the HLSC-CM revealed the presence of growth factors and cytokines with liver regenerative properties. In vitro experiments showed that HLSC-CM protected human hepatocytes from apoptosis and enhanced their proliferation. Conclusion: These data suggest that fulminant liver failure may potentially benefit from treatment with HLSCs or HLSC-CM. (HEPATOLOGY 2013)

Fulminant liver failure (FLF) is a life-threatening disease for which liver transplantation is the only definitive treatment (1), but the scarcity of donor livers and the timing of available organs often precludes transplantation. Liver regeneration could also be facilitated by using a bioartificial liver, but this approach is limited by the lack of availability of viable hepatocytes, required by the bioreactor (2). Stem cells, which can be expanded in vitro and cryopreserved, could form the basis of an ideal therapy (1). Liver stem cells, or even stem cells derived from other tissues, could potentially provide a source of human hepatocytes for regeneration of the injured liver (3, 4).

In particular, mesenchymal stem cells (MSCs), shown to be capable of in vitro differentiation into hepatocytes (5), were investigated as a possible source of hepatocytes for liver regeneration. In addition, it has been shown that secretion of trophic molecules by MSCs may favor regeneration following acute liver injury (6).

In a previous study, we isolated a population of human adult liver stem cells (HLSCs) expressing MSC markers and certain embryonic and hepatic cell markers, and having multipotent differentiation capabilities and regenerative properties (7). However, the therapeutic potential of HLSCs and HLSC-conditioned medium (CM) in FLF has not yet been evaluated. In this study we investigated the effect of HLSCs and HLSC-derived CM in a lethal model of liver injury induced by D-galactosamine (GalN) and lipopolysaccharide (LPS) in SCID mice.

Materials and Methods

Culture of HLSCs, MSCs, and Human Hepatocytes.

Human cryopreserved normal hepatocytes (n=3) were obtained from Lonza Bioscience (Basel, Switzerland) and were plated in the presence of alfa minimum essential medium/endothelial cell basal medium-1 (expansion media: α-MEM/EBM in the proportion 3:1, Lonza), supplemented with antibiotics (100 U penicillin and 1,000U streptomycin; both from Sigma, St. Louis) and 10% Foetal Calf Serum (FCS, Sigma). In this culture conditions, hepatocytes did not proliferate and died; after 2 week HLSC colonies were evident. At this time point, cells were expanded. The expanded cells were transferred to a T-75 flask and analyzed when they approached confluence. By FACS analysis HLSCs expressed MSCs specific markers (CD105, CD73, CD29 and Albumin) (Figure 5S) (7). Indirect immunofluorescence was performed on HLSCs as described (7). The following antibodies were used: albumin, α-fetoprotein (R&D Systems, Abington, U.K), vimentin, nestin (Sigma-Aldrich, St. Louis, MO), nanog, Oct3/4, sox2, musashi1, SSEA4 (all from Abcam, Cambridge, UK), cytokeratin-8 (Santa Cruz Biotechnology, Santa Cruz, CA), pax2 (Covance, Princeton, NJ), cytokeratin-18 (Chemicon International, Temecula, CA). HLSCs expressed specific hepatic markers (albumin, α-fetoprotein) and embryonic markers (nanog, Oct3/4, sox2, musashi1, SSEA4 and pax2) as shown in Figure 5S.

The MSCs, obtained from Lonza, were cultured in the presence of Mesenchymal Stem Cells Basal Medium (MSCBM, Lonza). To expand the MSCs, the adherent monolayer was detached by trypsin treatment for 5 minutes at 37° C, after 15 days for the first passage and every 7 days for subsequent passages. Cells were seeded at a density of 10,000 cells/cm^2 and used within the passage six.

All the MSC preparations (n=3) at different passages of culture expressed the typical MSC markers: CD105, CD73, CD44, CD90, CD166 and CD146. They also expressed HLA class I. MSC preparations did not express hematopoietic markers like CD45, CD14 and CD34. They also did not express the co-stimulatory molecules (CD80, CD86 and CD40). The adipogenic, osteogenic and chondrogenic differentiation ability of MSCs was determined as previously described (5).

Preparation of CM.

For the preparation of the CM, 2 x 10^5 HLSCs (passage 2-6) or MSCs (passage 2-6) were cultured in the presence of expansion media until 80% of confluence and further allowed to grow in α-MEM medium

supplemented with 2% FCS for 24 hours. For this purpose, cells were cultured in flasks of 75 cm^2 with 7 ml of media. The viability of cells incubated for 24 hours with 2% of FCS was for MSCs 95±4.3% and for HLSCs 96±3.2% as detected by trypan blue exclusion. The medium was concentrated at 4°C, approximately 25-fold, using ultrafiltration units (Amicon Ultra-PL 3, Millipore, MA, USA) with a 3 kDa molecular weight cut-off (6). After the concentration CM were kept at -20°C until use. The protein concentration of CM was determined by Bradford. All the CM were deprived of microvesicles (MVs) by ultracentrifugation (9).

Abbreviations

CM, conditional medium; FLF, fulminant liver failure; GalN, D-galactosamine; HLSCs, human liver stem cells; LPS, lipopolysaccharide; MSCs, mesenchymal stem cells.

The CM was analyzed for specific proteins, using multiplex biometric immunoassay, Bioclarma (Bio-Plex Human Cytokine Assay; Bio-Rad Laboratories, Hercules, CA) and data were confirmed by enzyme-linked immunosorbent assay (ELISA).

SCID Mice Model of FLF.

Studies were approved by the University of Torino Ethics Committee and conducted in accordance with the National Institutes of Health Guide for the Care and Use of Laboratory Animals. Intramuscular injection of Zolazepam (0.2 mL/kg) and Xilazin (16 mg/kg) were used as anesthesia (40 µL/mouse). FLF was induced in male SCID mice (7-8 weeks old) (Charles River Laboratories, Milan, Italy), by intraperitoneal injection of GalN (600 mg/kg body weight) and LPS (125 ng per animal) (10). Injection of GalN and LPS induced liver injury causing apoptosis and necrosis of hepatocytes with 100% lethality at 8 hours.

Thirty minutes after GalN/LPS administration, mice received different treatments. The following groups were studied: group 1, FLF mice intravenously injected with vehicle alone (n = 18); group 2, healthy mice intraperitoneally injected with vehicle instead of GalN/LPS (n = 6); group 3, FLF mice intravenously injected with 2 × 106 HLSCs (n = 9, 3.3 × 105 cells given six times for a total number of 2 × 106); group 4, FLF mice intravenously injected with 2 × 106 MSCs (n = 6, 3.3 × 105 cells given 6 times for a total number of 2 × 106); group 5, FLF mice intraperitoneally injected with 30 × 106 HLSCs (n = 9); group 6, FLF mice intraliver parenchyma (LP) injected (in the left lobe) with 0.5 × 106 (n = 5) or 0.2 × 106 HLSCs (n = 5); group 7, FLF mice intraperitoneally injected with concentrated HLSC-CM (n = 14); group 8, FLF mice intraperitoneally injected with concentrated MSC-CM (n = 5); group 9, FLF mice intraperitoneally injected with vehicle (PBS; n = 5); group 10, FLF mice intraperitoneally injected with concentrated HLSC-CM pretreated for 1 hour at 4°C with anti-HGF blocking antibody (100 mg/mouse; GeneTex, Aachen, Germany) (n = 5); group 11, FLF mice intraperitoneally injected with 25 ng/mouse of rhHGF (PreproTech, Rocky Hill, NJ,) (n = 5). The intravenous injection (120 mL) was performed in the vein of the tail within 30 seconds. In all experiments, cells cultured in T75 flasks until the 2-6 passage were detached by trypsin (0.5% w/v), washed, and resuspended in phosphate-buffered saline (PBS). Before in vivo injection, HLSCs were stained with the CellTrace CFSE Cell Proliferation Kit (Molecular Probes, Life Technologies, Paisley, UK) (11).

Morphologic Studies and Fluorescence In Situ Hybridization (FISH).

Liver samples were paraffin embedded or frozen for histology. For liver histology paraffin sections were stained with hematoxylin and eosin (H&E) (Merck, Darmstadt, Germany). All animals and all liver lobes were submitted to histology. Immunohistochemistry for detection of proliferation of liver cells was performed as described previously using anti-PCNA (Santa Cruz Biotechnology) antibody (8). Immunohistochemistry for HLSCs labelled with CFSE (Molecular Probes) in injured livers was conducted as described (11) using a anti-fluorescein/Oregon green antibody (Molecular Probes).

Apoptosis was also evaluated in paraffin embedded liver sections by TUNEL assay (ApopTag Apoptosis Detection Kit; Millipore Inc., Billerica, MA, USA).

Scoring for PCNA, CFSE and TUNEL-positive cells was carried out by counting the number of positive nuclei per field in 10 randomly chosen sections of liver using 40x magnification.

Confocal microscopy analysis (Zeiss LSM 5 Pascal; Carl Zeiss International) was performed on paraffin sections for detection of PCNA positive cells that co-expressed specific hepatocyte marker (pan-cytokeratin (Immunologycal sciences, Rome, IT) and or Cytokeratin8-18 (Genway Biotech. Inc, San Diego, CA) and of PCNA positive cells that were human (HLA-class I, Santa Cruz). Omission of the primary antibodies or substitution with non-immune rabbit or mouse IgG were used as controls. Alexa Fluor 488 anti-rabbit and Texas Red anti mouse (Molecular Probes) were used as secondary antibody. Nuclei were stained with Hoechst 33258 dye (Sigma)

Fluorescence in situ hybridization was performed using the pan-human centromeric probe (Vysis Inc., Downers Grove, IL). In situ hybridization was performed on 5-mm sections according to the manufacturer's guidelines. In brief, the sections were dewaxed in xylene, 2 times for 5 minutes each and rehydrated through graded alcohols to water for 5 minutes each. Slides were then incubated with sodium thiocyanate solution for 10 minutes at 80°C, washed in PBS 2 times for 5 minutes and incubated in Pepsin solution for 10 minutes at 37°C. Pepsin was quenched in glycine solution. Then sections were washed in PBS 2 times for 5 minutes and dehydrated through graded alcohols and air dry. Sections were denatured for 10 minutes at 80°C and hybridized with the probe (Pan centromeric chromosome paint human 1695 probe) for 16 to 18 hours at 37°C in HYBrite hybridization system (Vysis Inc.). As negative control, FISH was performed on liver sections of animal not injected with HLSCs.

Optical Imaging.

To evaluate the biodistribution of HLSCs, injected i.v (2x106) or L.P (0.2 and 0.5 x106), we performed Optical Imaging by Xenogen IVIS imaging system 200 Series (Caliper Life Sciences, Hopkinton, MA). The HLSC suspension was incubated in 20 uM Vybrant Cell Tracers DiD solution (Molecular Probes) following the manufacture's instruction. Cells were then in vivo injected (n=6). Images were acquired on organs collected 5-24 hours and 7 days after cell injection. Identical illumination settings were used for all image acquisitions. To control the background photon emission, the obtained data were subjected to average background subtraction, using an excitation of 535 nm. The photon radiance was expressed as photon per second per squared centimetre. The average radiance (p/sec/cm2/sr) was quantified in ROI (region of interest) drawn freehand. Images were analyzed using Living Images® software. Data were expressed as Average Radiance ±SD.

Apoptosis and Proliferation of Hepatocyte In Vitro.

In vitro apoptosis was evaluated by terminal TUNEL assay (Millipore) as previously described (8). Hepatocytes were cultured for 24 hours in 96-well plates at 30,000 cell/well in fibronectin coated plates. To

induced apoptosis, GalN was added at a concentration of 5 mM for 24 hours (8), followed by different doses of concentrated CM derived from HLSCs (29 µg/ml; 0.12- 0.46- 0.93 mg/ml). DNA synthesis was detected by incorporation of 5-bromo-2-deoxy-uridine (BrdU) into the cellular DNA (Roche Applied Science, Mannheim, Germany). Apoptosis and BrdU incorporation were evaluated in murine hepatocytes from control SCID mice or from mice after 30 minutes of induction of FLF in the same experimental condition explain above.

Statistical Analysis.

Data were analyzed using t tests, analysis of variance (ANOVA) with Newmann-Keuls' or ANOVA with Dunnett's multicomparison tests as appropriate. For survival experiments, a log-rank test was conducted. $P < 0.05$ was considered significant.

Results

HLSCs Improved Survival in a Model of FLF in SCID Mice.

The intraperitoneal administration of 600 mg/kg of GalN and 125 ng of LPS in SCID mice induced FLF with a 100% mortality rate within 8 hours (Fig. 1A). To evaluate whether HLSCs might rescue mice with FLF, the cells were administered 30 minutes after GalN/LPS-induced injury in different protocols: single intraperitoneal injection (3 × 107 cells); six repeated intravenous injections (3.3 × 105 cells, total: 2 × 106 cells); LP injection at two concentrations (0.2 and 0.5 × 106). Survival rates were 77%, 100%, and 100% in the case of intraperitoneal, intravenous, and LP injections, respectively (Fig. 1A,B). An equal number of MSCs was intravenously injected six times (3.3 × 105 cells, total: 2 × 106 cells) using the same protocol. The survival rate was 33% (Fig. 1A). Cell injection timings were chosen on the basis of preliminary experiments performed at 30 minutes, 1 and 4 hours, which showed that cell administration after 30 minutes did not improve survival.

Figure 1.

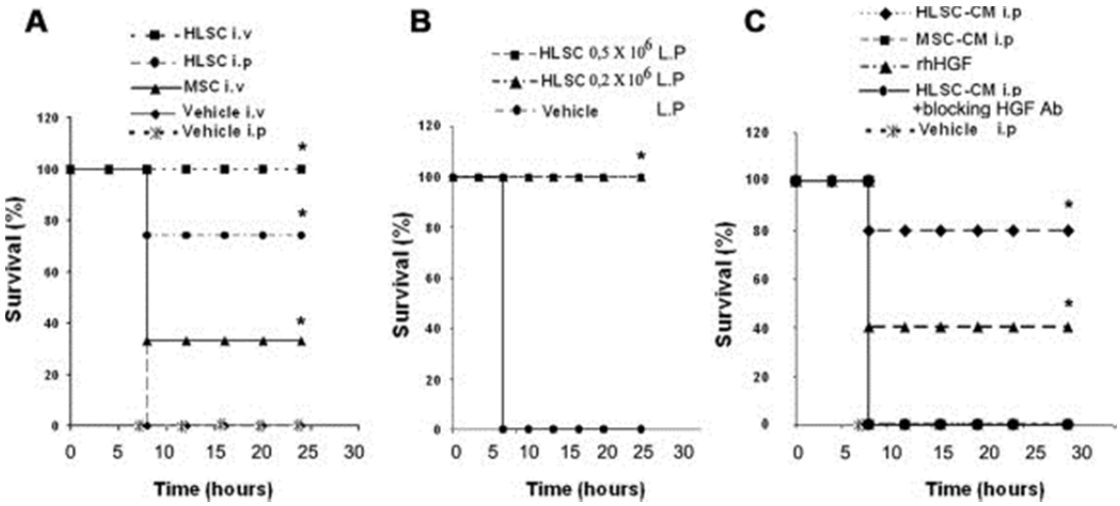

Effect of HLSCs on a SCID model of FLF induced by GalN/LPS. (A) After 30 minutes of injury induction, mice received intraperitoneal injection of vehicle (n = 6), intravenous injection of 2 × 106 HLSCs (n = 9), intravenous injection of 2 × 106 of MSC (n = 6), intraperitoneal injection of 30 × 106 HLSCs (n = 9), and intravenous injection of vehicle alone (n = 6). (B) Mice also received LP injections of 0.2 × 106 (n = 5), 0.5 × 106 (n = 5) of HLSCs and vehicle (n = 5). (C) Mice were inoculated intraperitoneally with vehicle,

250 μL of concentrated CM derived from HLSCs (n = 10) and 250 μL of concentrated CM derived from MSC (n = 5). Data were analyzed by a log-rank test: *P < 0.05 MSC intravenously, HLSCs intravenously versus vehicle (A); HLSCs 0.2 × 106 and 0.5 × 106 LP versus vehicle (B); HLSC-CM intraperitoneally, rhHGF versus HLSC-CM plus blocking antibody anti-HGF and vehicle (C). Liver functions and HLSCs localization in L.P mice with FLF. Alanine aminotransferase and aspartate aminotransferase were measured in serum of healthy SCID mice (Ctrl) and in FLF mice L.P. injected with 0.5 x 106 HLSCs and sacrificed 7, 14 or 21 days after injection. Data are expressed as mean ±SD U/L of five different SCID per group. Analysis of variance with Newman-Keuls multicomparison test was performed; *p<0.05 FLF mice L.P. injected with 0.5 x 106 HLSCs and sacrificed at 7 days vs Ctrl; #p<0.05 FLF mice L.P. injected with 0.5 x 106 HLSCs and sacrificed at 14 or 21 days vs FLF mice L.P. injected with 0.5 x 106 HLSCs and sacrificed at 7 days. (B) Quantification of CFSE+ cells per hpf (40x) in livers of healthy mice (white columns) and in liver of FLF mice L.P. injected with 0.5 x 106 HLSCs (black columns) and sacrificed 7 or 21 days after injection. (C) Quantification of fluorescence intensity, calculated in ROI, expressed as the mean of average radiance ±SD of mice L.P. injected with DiD labeled-HLSCs after induction of FLF (black bar). White bars are not treated control mice. Vehicle represent the intensity of liver of mice treated with PBS instead of HLSCs. Data are expressed as mean ±SD of 3 different SCID mice injected with HLSCs without FLF. (D) Representative fluorescence images of mice with or without FLF injury injected with DiD labeled-HLSCs and sacrificed after 24 hours 3 or 7 days. Abbreviations hours=h and days=d.

As paracrine mechanisms of adult stem cells were related to their secreted factors, we investigated and compared the effects of HLSC-CM and MSC-CM to that of HLSCs. As shown in Fig. 1C, the intraperitoneal injection of HLSC-CM induced an 80% survival. Conversely, MSC-CM did not protect mice from FLF. All controls treated with vehicle alone (PBS) died within 8 hours, suggesting that the effect on survival did not depend on mice hydration (Fig. 1C).

HLSCs Inhibited Liver Necrosis, Apoptosis and, Enhanced Liver Regeneration.

Histological analysis of mice treated with GalN/LPS showed extensive necrosis (Fig. 2A) and apoptosis (Fig. 3A) of the liver after 7 hours, along with a significant increase in liver enzyme levels measured in the peripheral blood (Fig. 2B,C). Treatment with intravenous injections of HLSCs led to a significant reduction of apoptosis and necrosis in surviving mice (Fig. 2A), despite the increase in liver enzymes at 7 hours. In mice surviving to injury, a significant decrease of liver enzymes was observed 3 days after HLSC injection, subsequently reaching normal values (Fig. 2B,C). A significantly lower concentration of ammonium was detected in serum of FLF mice (GalN/LPS) treated with HLSCs compared to vehicle alone (Fig. 2D). In HLSC-treated mice, normal liver morphology was reestablished after 7 to 21 days of treatment (not shown).

Figure 2.

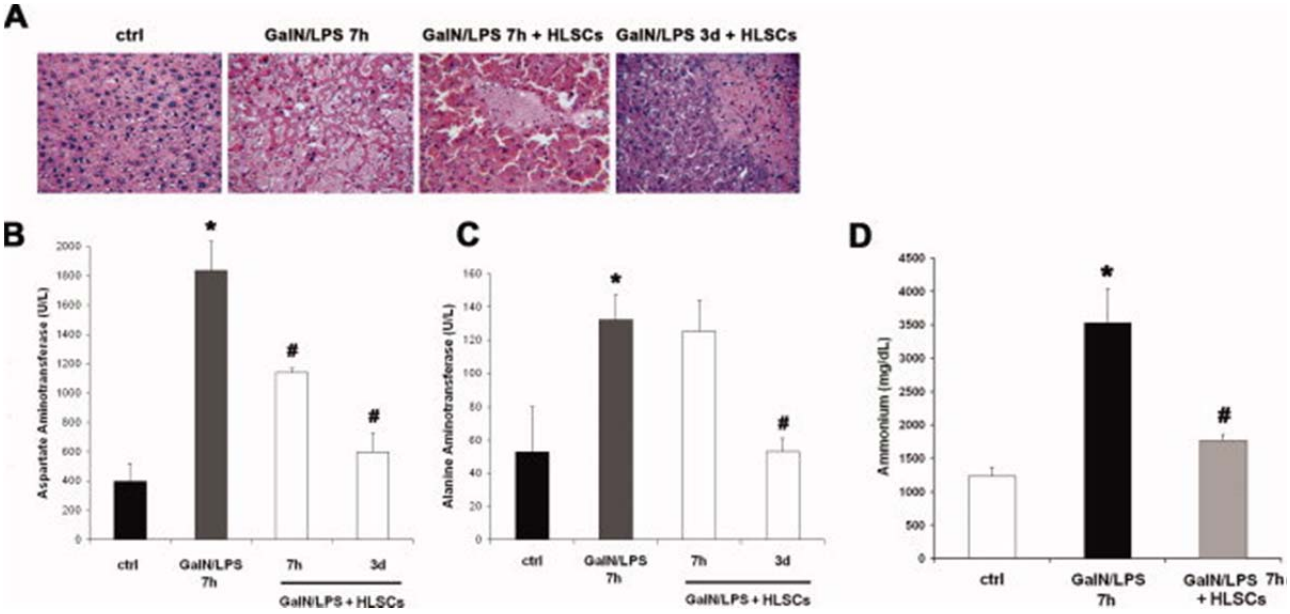

Effects of HLSCs on hepatic histomorphology and function in FLF mice. Representative light microscopy micrographs of liver histology at 7 hours and day 3 after induction of FLF in SCID mice treated or not with intravenous injection of 2 × 106 HLSCs. (A) H&E staining showing extensive cellular loss due to apoptosis and necrosis in FLF mice (GalN/LPS) at 7 hours with respect to control (ctrl). Cellular loss was reduced in FLF mice treated with HLSCs at 7 hours and especially after day 3. (B) Aspartate aminotransferase and alanine aminotransferase (C) were measured as biomarkers of liver cell injury in serum of control SCID mice (ctrl; black bar), in mice after 7 hours of FLF induction (gray bar) and in FLF mice treated with intravenous injection of 2 × 106 HLSCs and sacrificed 7 hours and day 3 after injury induction (white bar), and expressed as U/L. Data are expressed as mean ± standard deviation (SD) relative quantity of six different SCID per group. ANOVA with Newman-Keuls multicomparison test was performed; *P < 0.05 GalN/LPS after 7 hours versus ctrl; #P < 0.05 GalN/LPS injured SCID mice after 7 hours and day 3 of HLSC treatment versus GalN/LPS injured SCID mice. (D) Ammonium was measured in serum of vehicle-treated SCID mice (ctrl; white bar), in FLF mice after 7 hours (black bar), and in FLF mice treated with intravenous injection of 2 × 106 HLSCs and sacrificed at 7 hours (gray bar). Data are expressed as mean ± SD relative quantity. ANOVA with Newman-Keuls multicomparison test was performed; *P < 0.05 GalN/LPS after 7 hours versus ctrl; #P < 0.05 GalN/LPS injured SCID mice after 7 hours of HLSC treatment versus GalN/LPS injured SCID mice. Detection of HLSCs in spleens and lungs after in vivo injection. Representative micrographs of spleen and lung paraffin section of SCID mice injected with 2x106 of CFSE labeled HLSCs and stained with anti-CFSE antibody (brown staining). A small number of HLSCs were detectable within spleen and lung after 24 hours and 7 days, and disappeared after 21 days. Original Magnification x250. Abbreviations hours=h and days=d.

Figure 3.

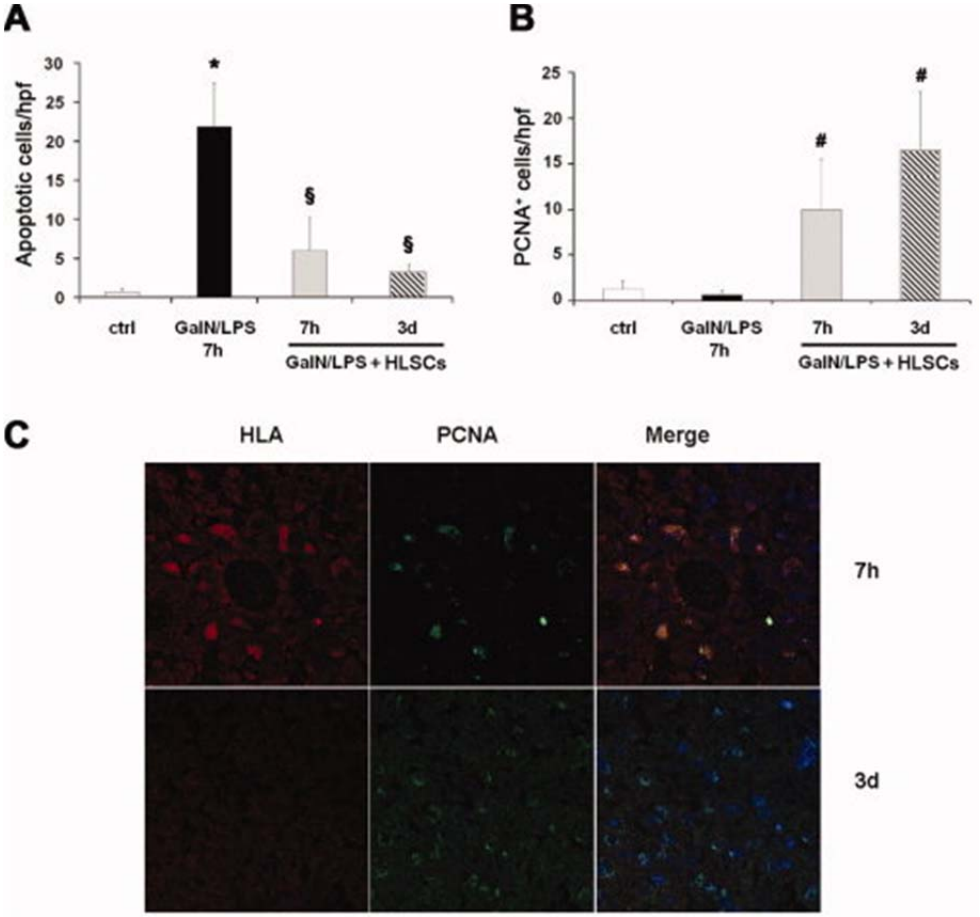

Effect of HLSCs on liver cell apoptosis and proliferation in FLF mice. (A) Quantification of apoptotic liver cells by TUNEL per high power field (hpf, 40×) in control mice injected with vehicle (white bars), in GalN/LPS mice after 7 hours (black bar), in GalN/LPS mice treated with intravenous injection of 2 × 106 HLSCs and sacrificed at 7 hours (gray bar) or day 3 (shaded bar). Data are expressed as mean ± SD relative quantity of three different mice per group. ANOVA with Newman-Keuls multicomparison test was performed; *P < 0.05 GalN/LPS injured SCID mice after 7 hours versus vehicle; §P < 0.05 GalN/LPS mice treated with intravenous injection HLSCs at 7 hours or 3 days versus GalN/LPS injured SCID mice after 7 hours. (B) Quantification of PCNA+ liver cells per hpf (40×) in control mice injected with vehicle (white bars), GalN/LPS injured SCID mice after 7 hours (black bar), in GalN/LPS mice treated with intravenous injection of 2 × 106 HLSCs and sacrificed at 7 hours (gray bar) or day 3 (shaded bar). Data are expressed as mean ± SD relative quantity of three different mice per group. ANOVA with Newman-Keuls multicomparison test was performed; #P < 0.05 GalN/LPS mice treated with intravenous injection HLSCs at 7 hours or day 3 versus GalN/LPS mice after 7 hours. (C) Representative immunofluorescence showing coexpression of HLA and PCNA at 7 hours and 3 days (d). Original magnification 400×. In vitro effect of HLSCs-CM on murine hepatocytes. (A) Apoptosis was evaluated by Tunel assay on murine hepatocytes incubated with vehicle alone (white column) in the presence of GalN 5mM (black column) and in the presence of 29 μg/ml of concentrated HLSC-CM (grey column). (B) Proliferation evaluated by BrdU incorporation on murine hepatocytes incubated with vehicle alone (black column) or with different concentrations of concentrated HLSC-CM (29 μg/ml; 0.12-0.46-0.93 mg/ml) (grey columns). (C) Apoptosis performed on murine hepatocytes isolated from mice after 30 minutes from induction of FLF (white column) and cultured in the presence or absence 29 μg/ml of CM (black column). Results are expressed as mean ±SD of three different experiments performed in triplicate. Analyses of variance with Newmann-Keuls multicomparison test was performed; *p<0.05 hepatocytes incubated with GalN 5mM versus vehicle alone; #p<0.05 hepatocytes incubated with 29 μg/ml of concentrated HLSC-CM vs hepatocytes incubated with GalN 5mM. (A and C). (D) Proliferation evaluated by BrdU incorporation on murine hepatocytes isolated from mice after 30 minutes from induction of FLF cultured in the presence of vehicle alone (black columns) or with different concentration of concentrated HLSC-CM (grey columns). Results are expressed as mean ±SD of three different experiments performed in triplicate. Analyses of variance with Newmann-Keuls multicomparison test was performed; *p<0.05 hepatocytes incubated with 0.46; 0.93 mg/ml of CM vs hepatocytes incubated with vehicle alone (B and D).

As shown in Fig. 3, HLSCs significantly inhibited liver apoptosis in FLF mice (GalN/LPS) compared to vehicle alone. Proliferating cell nuclear antigen (PCNA)-positive cells detected at 7 hours expressed human leukocyte antigen (HLA) or CFSE, indicating that they were derived from the injected HLSCs (Fig. 3C). However, after 3 days in mice treated with HLSCs, PCNA-positive cells were mainly negative for HLA and CFSE, indicating that most proliferating cells were of murine origin (Fig. 3C).

Intravenous- and LP-Injected HLSCs Localized in the Liver of FLF Mice.

Liver cell localization was evaluated by IVIS using DiD-labeled HLSCs (12, 13). As shown in Fig. 4A,B, after intravenous injection HLSCs preferentially accumulated in livers of mice with FLF but not in livers of healthy mice (Fig. 4A,B). Fluorescence signals, expressed as average radiance, increased until day 7 in livers of mice with FLF but not in those of healthy mice. In LP-injected mice, no difference in liver accumulation of HLSCs between FLF and healthy mice was observed (Fig. 1S,B).

Figure 4.

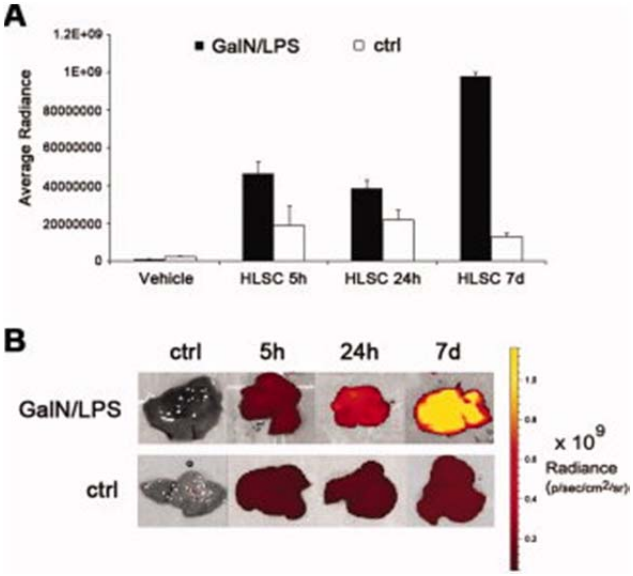

Liver localization of HLSCs by IVIS. (A) Quantification of fluorescence intensity, calculated in region of interest (ROI), expressed as the mean of average radiance ± SD of mice injected with DiD-labeled HLSCs after induction of FLF (black bar) or not (white bars). Vehicle represents the intensity of liver of mice treated with PBS instead of HLSCs. Data are expressed as mean ± SD of two SCID mice injected with HLSCs after induction of FLF and ± SD of four SCID mice injected with HLSCs without FLF. (B) Representative fluorescence images of mice with or without FLF injury injected with DiD-labeled HLSCs and sacrificed after 5, 24 hours, or day 7. Bioclarma assay. A multiplex biometric immunoassay, Bioclarma was used to quantify the amount of cytokines contained in HLSC-CM and in MSC-CM. Data are expressed as ng/ml and as mean ±SD of three different experiments performed in duplicate. A) High expressed cytokines and growth factors; B) low expressed cytokines and growth factors. Analysis of variance with Newman-Keuls multicomparison test was performed; *p<0.05 HLSC-CM vs MSC-CM; #p<0.05 MSC-CM vs HLSC-CM.

By immunohistochemistry, CFSE-labeled HLSCs were mainly detected in large liver vessel walls after 24 hours and within the liver parenchyma after days 7 and 21 in intravenously injected surviving FLF mice (Fig. 5A,D,E). In these mice, CFSE-labeled HLSCs were transiently detected after 24 hours in lungs and spleens, decreasing thereafter (Fig. 5B,C; Fig. 2S). When HLSCs were intravenously injected in healthy mice treated with vehicle alone, liver accumulation was significantly lower than in FLF mice (Fig. 5A). In LP-injected mice,

CFSE-labeled HLSCs were detected in the liver parenchyma at days 7 and 21 following injection (Fig. 1S,B), but there was no accumulation in lungs or spleens at any timepoint (not shown).

Figure 5.

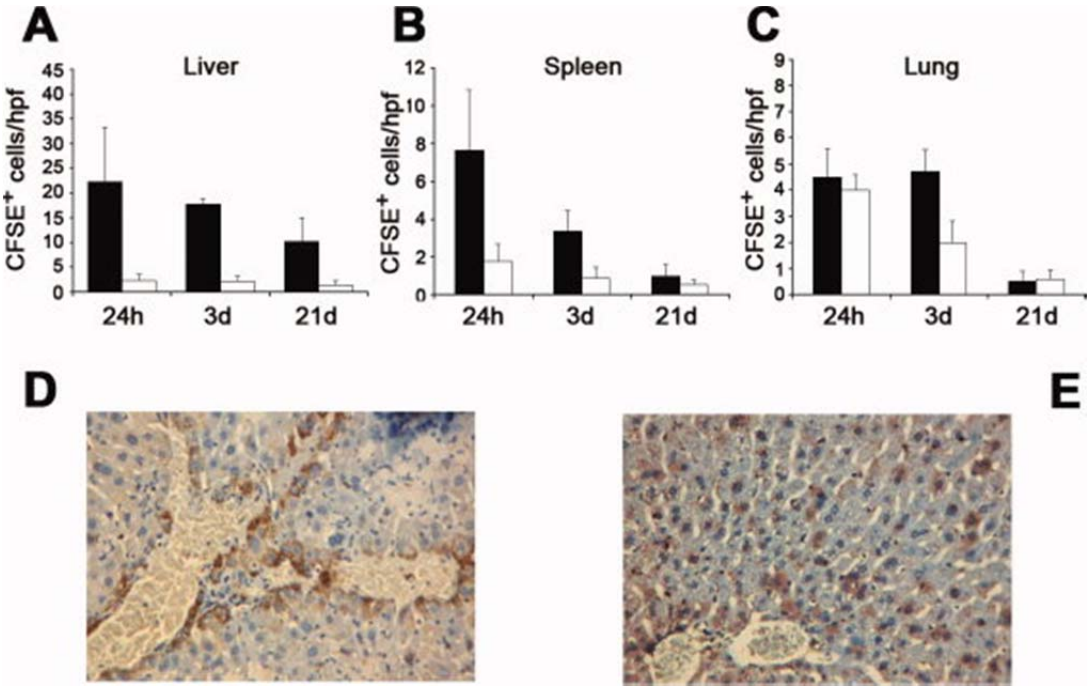

Detection of HLSCs after in vivo injection. (A-C) Quantification of CFSE+ cells per hpf (40×) in livers, spleens, and lungs of SCID mice injected with 2 × 106 of CFSE-labeled HLSCs after induction of FLF (black bars) or not (white bars). Data are expressed as mean ± SD of relative quantity of cells in three different mice per group. (D,E) Representative micrographs of livers paraffin section of SCID mice injected with 2 × 106 of CFSE-labeled HLSCs and stained with anti-CFSE antibody (brown staining). HLSCs were detectable within liver large vessels after 24 hours (D) and after day 7 (E) and 21 (not shown) within the liver parenchyma. Characterization and potency of HLSC. (A) Representative confocal micrographs showing expression of several embryonic, mesenchymal stem cells and hepatic markers on HLSCs. (B) FACS analysis of HLSC showing the expression of CD105, CD73, CD29 and albumin. (C) Urea production by HLSCs in RCCS at different time-points was evaluated and compared with that of HLSCs cultured in adhesion with growth factors. Data are expressed as mg/dL and as mean ±SD of three different experiments. ANOVA was performed; *p<0.05 HLSCs cultured in RCCS vs HLSCs cultured in adhesion.

In Vivo Expression of Mature Hepatic Markers by HLSCs.

To assess whether HLSCs engrafted in the liver expressed mature hepatic markers, we investigated coexpression of human antigen HLA and mature hepatic markers such as cytokeratin 8 and 18 by confocal analysis (Fig. 6). At day 7 the majority of HLA-positive cells expressed cytokeratin 8 and 18 (Fig. 6A,B). At day 21, ~50% of HLA-positive cells expressed cytokeratin 8/18 (Fig. 6A,B). FISH analysis with the human pan-centromeric probe showed that at 24 hours positive cells were pan-cytokeratin-negative, whereas at days 7 and 21 they coexpressed pan-cytokeratin and human chromosome (Fig. 6B). At day 21 several pan-centromeric-positive cells did not express pan-cytokeratin, suggesting that some undifferentiated HLSCs were still present in liver parenchyma (Fig. 6B).

Figure 6.

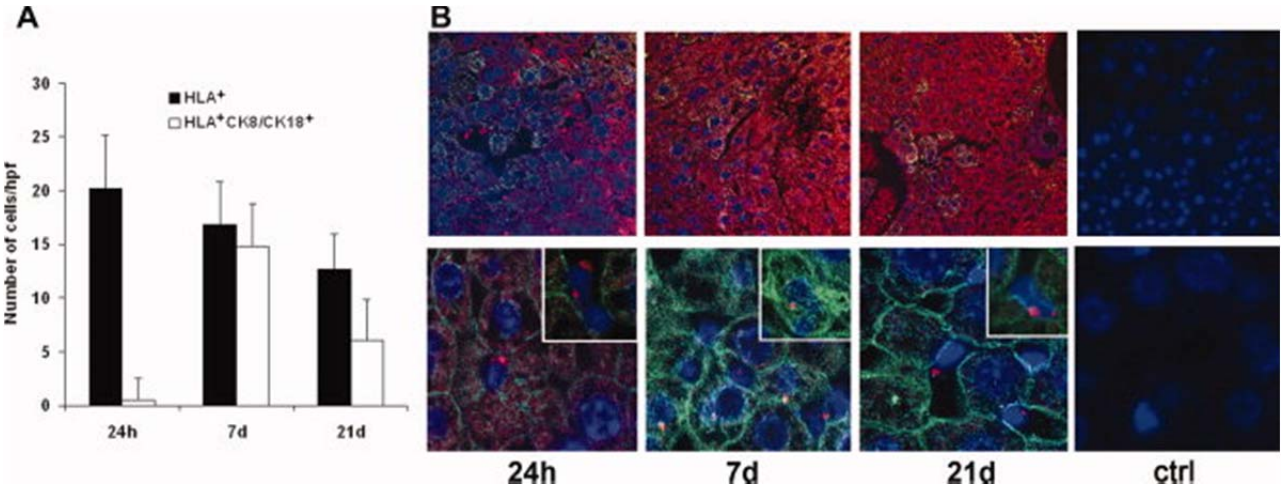

In vivo differentiation of HLSCs. (A) Number of HLSCs engrafted in liver of GalN/LPS mice treated with intravenous injection of 2 × 106 HLSCs and sacrificed at 24 hours, 7, and 21 days detected as HLA+ cells (black columns), or HLA+CK8/18+ cells (white columns). (B) Representative confocal micrographs showing in the upper panel the intraparenchymal localization of HLSCs by the expression of HLA class I (green) and of cytokeratin 8 and 18 (red) in liver sections of SCID mice after induction of FLF treated with HLSCs or not and sacrificed 24 hours, 7, or 21 days later. Ctrl = isotypic control. Original magnification: 400×. Representative confocal micrographs showing in the lower panel FISH analysis performed with human pan-centromeric probe (red spots) costained with pan-cytokeratin (green fluorescence). Ctrl = FISH analysis on normal murine liver. Nuclei were counterstained with Hoechst dye. Original magnification: 630×.

HLSC-CM Inhibited Liver Necrosis and Apoptosis and Enhanced Liver Regeneration.

In the GalN/LPS model of FLF, HLSC-CM showed a similar protective activity on liver function and morphology compared to HLSCs (Figs. 1C, 7A,B). The increased presence of PCNA-positive cells demonstrated liver regeneration in mice treated with HLSC-CM (Fig. 7C) and apoptosis was significantly reduced compared to mice treated with vehicle alone (Fig. 7D).

Figure 7.

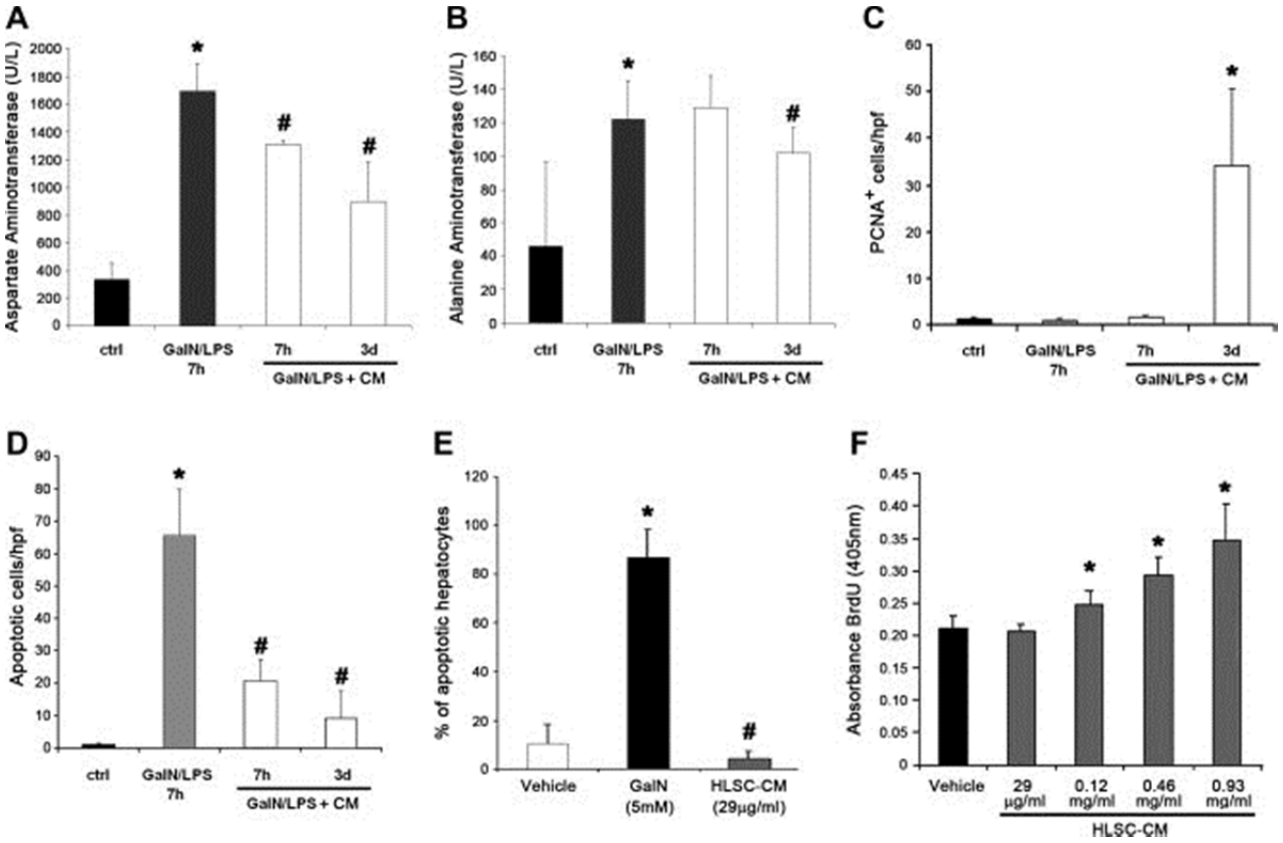

In vivo and in vitro effect of HLSC-CM. Alanine aminotransferase (A) and aspartate aminotransferase (B) were measured in serum of vehicle-treated mice (ctrl; black bar), of GalN/LPS injured mice after 7 hours (gray bar) and GalN/LPS mice after 7 hours treated with intraperitoneal injection of 250 µL of concentrated HLSC-CM and sacrificed 7 hours and 3 days (white bar), and expressed as U/L. Data are expressed as mean ± SD relative quantity of three mice per group. ANOVA with Newman-Keuls multicomparison test was performed; *P < 0.05 GalN/LPS after 7 hours versus ctrl; #P < 0.05 HLSC-CM injected SCID mice after GalN/LPS injury versus GalN/LPS mice after 7 hours and day 3. (C) Quantification of PCNA+ liver cells per hpf (40×) in control mice injected with vehicle (black bar), in GalN/LPS mice after 7 hours (gray bar), and in GalN/LPS mice treated with i.p injection of 250 µL of concentrated HLSC-CM and sacrificed after 7 hours and 3 days (white bars). Data are expressed as mean ± SD relative quantity of three mice per group. ANOVA with Newman-Keuls multicomparison test was performed; *P < 0.05 HLSC-CM treated GalN/LPS injured SCID mice after 3 days versus GalN/LPS injured SCID mice. (D) Quantification of apoptotic+ liver cells per hpf (40×) in control mice injected with vehicle (black bar), in GalN/LPS mice after 7 hours (gray bar), and in GalN/LPS mice treated with intraperitoneal injection of 250 µL of concentrated HLSC-CM and sacrificed after 7 hours and 3 days (white bars); Data are expressed as mean ± SD of relative quantity of cells in three mice per group. ANOVA with Newman-Keuls multicomparison test was performed; *P < 0.05 GalN/LPS injured SCID mice after 7 hours versus vehicle; #P < 0.05 HLSC-CM treated GalN/LPS mice after 7 hours and day 3 versus GalN/LPS mice. (E) In vitro apoptosis was evaluated by TUNEL assay in human hepatocytes incubated with vehicle alone (white bars) in the presence of GalN 5mM (black bar) and in hepatocytes incubated with 29 µg/mL of concentrated HLSC-CM (gray bars). Results are expressed as mean ± SD of three different experiments performed in triplicate. ANOVA with Newman-Keuls multicomparison test was performed; *P < 0.05 hepatocytes incubated with GalN 5 mM versus vehicle alone; #P < 0.05 hepatocytes incubated with 29 µg/mL concentrated HLSC-CM versus hepatocytes incubated with GalN 5 mM. (F) Proliferation was evaluated by bromodeoxyuridine (BrdU) incorporation in hepatocytes cultured in the presence of vehicle alone (black bar) or with different concentration of concentrated HLSC-CM (29 µg/mL; 0.12-0.46-0.93 mg/mL) (gray bars). Results are expressed as mean ± SD of three different experiments performed in triplicate. ANOVA with Newman-Keuls multicomparison test was performed; *P < 0.05 hepatocytes incubated with 0.12, 0.46, and 0.93 mg/mL of concentrated HLSC-CM versus hepatocytes incubated with vehicle alone.

In vitro studies confirmed that HLSC-CM at doses as low as 29 µg protein/mL protected human hepatocytes from GalN-induced apoptosis (Fig. 7E). Moreover, increasing concentrations of HLSC-CM enhanced proliferation of human hepatocytes (Fig. 7F). Similar results were obtained with murine hepatocytes isolated from both normal and FLF mice (Fig. 3S)

As shown in Table 1 and Fig. 4S, HLSC-CM contained several growth factors/cytokines potentially involved in liver protection and regeneration, the most represented of which were interleukin (IL)-6, IL-8, vascular endothelial growth factor (VEGF), hepatocyte growth factor (HGF), and MSP, reconfirmed by single ELISA. The concentration of HGF in HLSC-CM was ~50-fold higher than in MSC-CM. Treatment of HLSC-CM with neutralizing antihuman HGF antibody abrogated the protective effect of HLSC-CM (Fig. 1C), and the survival rate of mice treated with rhHGF was ~40%, suggesting a relevant role of HGF in the hepatoprotective effect of HLSC-CM (Fig. 1C).

Table 1. Concentration of Cytokines (ng/mL)

Cytokines	2%FCS	HLSCs		MSCs	
	ELISA	Bioclarma	ELISA	Bioclarma	ELISA
VEGF	0	119 ± 56	119 ± 79	158 ± 5	158 ± 7
HGF	0	52 ± 12	52 ± 17	0.46±0.2	0
IL-6	0.034±0.01	38 ± 4	37.9 ± 6.2	30 ± 3	30.4 ± 4.9
IL-8	0	207 ± 15	207 ± 20.5	228 ± 13	228 ± 17.7
MCP1	0	5.7 ± 0.2	5.68 ± 0.27	5.5 ± 0.5	5.49 ± 0.66
MSP1	0	34.4 ± 28	34.4 ± 39.6	0	0

We also evaluated the amount of human and murine VEGF, IL-6, and HGF in SCID mice with FLF after intravenous injection with HLSCs. Human HGF and IL-6 levels in mouse serum peaked at 7 hours after HLSC injection (hIL6 = 596 ± 390 pg/mL; hHGF = 482 ± 370 pg/mL), decreased after 24 hours (hIL6 = 46 ± 19 pg/mL; hHGF = 2 ± 1.6 pg/mL), and were undetectable after day 7. Human VEGF was undetectable. In mice injected with HLSCs, murine HGF was not significantly different from untreated controls (respectively 101 ± 49 pg/mL versus 107 ± 19 pg/mL). An increase of murine HGF (159 ± 106 pg/mL) was observed after 24 hours, decreasing thereafter. Levels of murine VEGF and IL-6 did not increase at any time after HLSC administration.

Discussion

The results of our study can be summarized as follows: (1) HLSCs and HLSC-CM strikingly improved survival and reduced plasma levels of liver enzymes and ammonium in mice with FLF, and (2) the protective effect of HLSCs and HLSC-CM was due to reduced apoptosis, necrosis, and enhanced proliferation.

Cell therapy based on hepatocyte transplantation is a potential treatment option in patients with acute liver failure (14). Transplanted hepatocytes may replace liver functions allowing endogenous regeneration. However, the availability of a suitable cellular source is a limiting factor, but stem cells could represent an ideal cell source for liver regeneration. The capacity of stem cells to reverse liver injury has been shown in different experimental models of liver failure, e.g., in a liver fibrosis model induced by carbon tetrachloride (CCl_4), mice treated with MSCs presented less fibrosis, better liver function, and a significant improvement

of survival compared to untreated mice (15, 16). In addition, MSCs were shown to protect the liver against hepatocyte apoptosis induced by ischemia-reperfusion injury, and to enhance liver regeneration (9).

Recently, Parekkadan et al. (6) demonstrated that intravenous injection of MSC-CM or extracorporeal perfusion in a bioreactor containing MSCs had a significant survival benefit in treatment of FLF in rats. Zagoura et al. (17) reported that human amniotic fluid-derived MSCs also led to liver repair in a model of CCl4-induced acute hepatic injury. In particular, repair was increased when MSCs were initially differentiated in vitro into hepatic progenitor-like cells. Despite the observation of engraftment of the injected cells, a relevant role for secreted molecules was suggested (17).

In the present study we showed that HLSCs may have a therapeutic potential in a lethal model of FLF in SCID mice. Enhanced survival and the improved histopathological findings were associated with significantly lower plasma serum transaminases and ammonium levels. HLSCs are liver-resident MSCs that are already committed to a hepatic lineage, thus do not require in vitro differentiation (7). Immunofluorescence tracing as well as FISH analyses using a human pan-centromeric probe showed some HLSC engraftment within the liver. Coexpression of pan-cytokeratin and human centromere indicated that at day 7 the majority of engrafted HLSCs expressed pan-cytokeratin, with a significantly reduced expression at day 21. This suggests the persistence of an undifferentiated, small population of human HLSCs. However, our hypothesis is that recovery by HLSCs is attributed to a paracrine mechanism, and not by the substitution of the injured parenchyma. In fact, repopulation of the liver was mainly dependent on proliferation of murine hepatocytes. Crucially, HLSC-CM, containing several cytokines with proproliferative and antiapoptotic properties mimicked the effect of HLSCs. Contrary to other experimental models of liver injury, MSC-CM was totally ineffective in the present model. Comparing the composition of HLSC-CM and MSC-CM, HGF was found to be ~50-fold higher in HLSC-CM than in MSC-CM, which prompted us to perform in vivo experiments using rhHGF or HGF blockade, demonstrating that the beneficial effect of HLSC-CM depended, at least partly, on HGF.

These results suggest that in liver regeneration, hepatocyte proliferation is sustained by soluble factors. In this context, Strick-Marchand et al. (18) recently showed a beneficial crosstalk between the immune system and liver stem cells that operates through the release of cytokines that could promote tissue regeneration following acute liver damage. Moreover, Van Poll et al. (19) demonstrated a direct antiapoptotic and promitotic effect of MSC-CM in vitro and Parekkadan et al. (6) demonstrated that the MSC-induced improvement in survival was attributed to antiinflammatory chemokine release in a rat model of GalN-induced FLF.

In the present study we found that some HLSCs, unlike MSCs, persisted in the liver after days 7 and 21. However, the observation that cell-free HLSC-CM mimicked the HLSC effects suggests a paracrine action by the release of cytokines and growth factors. Interestingly, HLSC-CM inhibited in vitro hepatocyte death and stimulated proliferation, and ELISA analysis of the HLSCs-CM showed the presence of several growth factors/cytokines, potentially involved in liver regeneration. In particular, HLSC-CM contained liver protective factors, such as IL-10 (an antiinflammatory cytokine, recently identified as a mediator of the hepatoprotective action of amniotic fluid-derived hepatic progenitor cells), IL-1ra, MCP-1, and IL-1 beta (6, 17) HLSCs also secrete growth factors such as VEGF, which facilitates angiogenesis and is involved in tissue repair (21, 22), and IL-8, a chemokine with proangiogenic activity (23). In HLSC-CM, we also found growth factors with known hepatoprotective properties, such as HGF, IGF-1, and IL-6 (24) However, the growth factor of greatest relevance is HGF in HLSC-CM (only expressed at low levels in MSC-CM), as blocking HGF significantly prevented the protective effect of HLSC-CM, and stimulation with rhHGF improved survival.

In conclusion, HLSCs and HLSC-CM may improve survival in a lethal mouse model mainly by paracrine mechanisms, and HLSCs may therefore represent a new cell source for FLF treatment.

Referernces

1. Russo FP, Parola M. Stem and progenitor cells in liver regeneration and repair. Cytotherapy. 2011; 13: 135-144.

2. Kobayashi N, Okitsu T, Tanaka N. Cell choice for bioartificial livers. Keio J Med 2003; 52: 151-157.

3. Oertel M, Shafritz DA. Stem cells, cell transplantation and liver repopulation. Biochim Biophys Acta 2008; 1782: 61-74.

4. Stock P, Brückner S, Ebensing S, Hempel M, Dollinger MM, Christ B. The generation of hepatocytes from mesenchymal stem cells and engraftment into murine liver. Nat Protoc 2010; 5: 617-627.

5. Piryaei A, Valojerdi MR, Shahsavani M, Baharvand H. Differentiation of bone marrow-derived mesenchymal stem cells into hepatocyte-like cells on nanofibers and their transplantation into a carbon tetrachloride-induced liver fibrosis model. Stem Cell Rev 2011; 7: 103-118.

6. Parekkadan B, van Poll D, Suganuma K, Carter EA, Berthiaume F, Tilles AW, et al. Mesenchymal stem cell-derived molecules reverse fulminant hepatic failure. PLoS One 2007; 2: e941.

7. Herrera MB, Bruno S, Buttiglieri S, Tetta C, Gatti S, Deregibus MC, et al. Isolation and characterization of a stem cell population from adult human liver. Stem Cells 2006; 24: 2840-2850.

8. Herrera MB, Fonsato V, Gatti S, Deregibus MC, Sordi A, Cantarella D, et al. Human liver stem cell-derived microvesicles accelerate hepatic regeneration in hepatectomized rats. J Cell Mol Med 2010; 14: 1605-1618.

9. Kanazawa H, Fujimoto Y, Teratani T, Iwasaki J, Kasahara N, Tsuruyama T, et al. Bone marrow-derived mesenchymal stem cells ameliorate hepatic ischemia reperfusion injury in a rat model. PLoS One 2011; 296: e19195.

10. Lehmann V, Freudenberg MA, Galanos C. Lethal toxicity of lipopolysaccharide and tumor necrosis factor in normal and D-galactosamine-treated mice. J Exp Med 1987; 165: 657-663.

11. Herrera MB, Bussolanti B, Bruno S, Morando L, Mauriello-Romanazzi G, Sanavio F, et al. Exogenous mesenchymal stem cells localize to the kidney by means of CD44 following acute tubular injury. Kidney Int 2007; 72: 430-441.

12. Boddington SE, Sutton EJ, Henning TD, Nedopil AJ, Sennino B, Kim A, et al. Labeling human mesenchymal stem cells with fluorescent contrast agents: the biological impact. Mol Imaging Biol 2011; 13: 3-9.

13. Sutton EJ, Boddington SE, Nedopil AJ, Henning TD, Demos SG, Baehner R, et al. An optical imaging method to monitor stem cell migration in a model of immune-mediated arthritis. Opt Express 2009; 17: 24403-24413.

14. Dhawan A, Puppi J, Hughes RD, Mitry RR. Human hepatocyte transplantation: current experience and future challenges. Nat Rev Gastroenterol Hepatol 2010; 7: 288-298.

15. Cho KA, Lim GW, Joo SY, Woo SY, Seoh JY, Cho SJ, et al. Transplantation of bone marrow cells reduces CCl4-induced liver fibrosis in mice. Liver Int 2011; 31: 932-939.

16. Sakaida I, Terai S, Yamamoto N, Aoyama K, Ishikawa T, Nishina H, et al. Transplantation of bone marrow cells reduces CCl4-induced liver fibrosis in mice. HEPATOLOGY 2004; 40: 1304-1311.

17. Zagoura DS, Roubelakis MG, Bitsika V, Trohatou O, Pappa KI, Kapelouzou A, et al. Therapeutic potential of a distinct population of human amniotic fluid mesenchymal stem cells and their secreted molecules in mice with acute hepatic failure. Gut 2012; 61: 894-906.

18. Strick-Marchand H, Masse GX, Weiss MC, Di Santo JP. Lymphocytes support oval cell-dependent liver regeneration. J Immunol 2008;18:2764-2771.

19. Van Poll D, Parekkadan B, Cho CH, Berthiaume F, Nahmias Y, Tilles AW, et al. Mesenchymal stem cell-derived molecules directly modulate hepatocellular death and regeneration in vitro and in vivo. HEPATOLOGY 2008; 47: 1634-1643.

20. Bao P, Kodra A, Tomic-Canic M, Golinko MS, Ehrlich HP, Brem H. The role of vascular endothelial growth factor in wound healing. J Surg Res 2009; 153: 347-358.

21. Tögel F, Zhang P, Hu Z, Westenfelder C. VEGF is a mediator of the renoprotective effects of multipotent marrow stromal cells in acute kidney injury. J Cell Mol Med 2009; 13: 2109-2114.

22. Martin D, Galisteo R, Gutkind JS. CXCL8/IL8 stimulates vascular endothelial growth factor (VEGF) expression and the autocrine activation of VEGFR2 in endothelial cells by activating NFkappaB through the CBM (Carma3/Bcl10/Malt1) complex. J Biol Chem 2009; 284: 6038-6042.

23. Hoek JB, Pastorino JG. Ethanol, oxidative stress, and cytokine-induced liver cell injury. Alcohol 2002; 27: 63-68.

24. Li WC, Ralphs KL, Tosh D. Isolation and culture of adult mouse hepatocytes. Methods Mol Biol 2010; 633: 185-196.